RESEARCH PAPER

CrossMark

Characterization of a nanoflow sheath liquid interface and comparison to a sheath liquid and a sheathless porous-tip interface for CE-ESI-MS in positive and negative ionization

Oliver Höcker[1] · Cristina Montealegre[1] · Christian Neusüß[1]

Abstract
Coupling of capillary electrophoresis to electrospray mass spectrometry still remains challenging and a topic of research to find the best interface regarding sensitivity, robustness, and ease of use. Here, a nanoflow sheath liquid interface for CE-ESI-MS is presented and compared to both a standard triple-tube sheath liquid and a porous-tip sheathless interface for three groups of analytes. The nanoflow sheath liquid interface with a separation capillary inserted into a glass emitter was initially characterized to facilitate optimization and method development. Implementation of a shut-off valve, syringe pump, and inline filter enabled easy handling and fast analyses, repeatable both in positive and negative modes (intra-day RSD of 6.6 to 12.0%). The same setup was used for sheathless interfacing by exchanging the emitter and using a porous etched tip separation capillary. Both nanoflow interfaces showed similar performance. Average peak areas using the nanoflow sheath liquid interface were a factor of 38 for 6 organic acids in negative mode, 114 and 36 for the light and heavy chain of a monoclonal antibody, and 13 higher for peptides in positive mode compared to the triple-tube interface. This first direct comparison of the three most common interfaces exhibits a strong improvement in sensitivity to the same extent for both nanoflow interfaces, where sheath liquid interfaces offer full flexibility in method development.

Keywords Capillary electrophoresis/electrophoresis · Mass spectrometry · Electrospray ionization · Interfacing

Introduction

The hyphenation of capillary electrophoresis (CE) with mass spectrometry (MS) is a valuable technique for the analysis of charged compounds in a wide field of application like proteomics, metabolomics, drug analysis, and bioanalysis as well as in food and forensic sciences [1]. The commercially available co-axial sheath liquid electrospray (ESI) interface is used for routine analyses in many applications due to its robustness and analytical stability [2]. However, utilization of sheath liquid flow rates of 1 to 10 μL/min dilutes the low-flow CE

✉ Christian Neusüß
Christian.Neusuess@hs-aalen.de

[1] Department of Chemistry, Aalen University, Beethovenstrasse 1, 73430 Aalen, Germany

effluent and decreases sensitivity, wherefore nanoflow electrospray ionization represents an alternative. Nanoflow electrospray interfaces are characterized by the use of small ID emitters and flow rates below 1000 nL/min [3] omitting a nebulizing gas. In this regime, comparably smaller initial droplets are produced, thus generating gas phase ions more efficiently and the tip can be positioned closer to the MS orifice to enhance sampling [4]. In the last years, several new designs appeared in the literature, aiming at the enhancement of sensitivity while trying to maintain reproducibility and robustness, demonstrating the relevance of the topic. Recent reviews summarize the properties of the interfaces and study the principles of ESI and nanoESI concepts [3, 5–8].

Sheathless interfacing benefits from the absence of additional liquid diluting the capillary effluent by spraying the background electrolyte (BGE) directly, resulting in high ionization efficiencies. The lack of supporting liquid can compromise separation and electrospray conditions, since pH value, electroosmotic flow (EOF), capillary coating, organic solvent,

🖄 Springer

or inlet pressure need to be considered to achieve an effective spray. The electrical contact for grounding can be realized in various ways, leading to different designs reported in the literature, for example a sheathless porous-tip interface [9], by using a detachable porous emitter [10, 11], a metal-coated emitter [12], a sub-micrometer fracture in the capillary for the electrical contact [13], or an "interface-free" approach by using a narrow capillary with an ID ≤ 15 μm omitting an additional power supply or grounding [14]. The sheathless porous-tip interface, introduced in 2007 by Moini [9], is based on a 30-μm capillary etched to porosity to close the electrical contact over the conductive liquid. This interface has been commercialized by Beckman Coulter (now Sciex, Brea, California, USA) and, thus, has been used by several research groups. LODs in nanomolar to picomolar concentrations have been reported for anionic metabolites [15] or intact proteins [16]. Comparisons with the triple-tube sheath liquid interface demonstrated an improvement of at least 8–30 times for the analysis of the urinary metabolome [17], 50–140 times lower LODs for intact proteins [18], and improvements of more than fivefold in intensity and 10 times higher number of peaks detected for cationic metabolites [19].

Nanoflow sheath liquid interfaces operate in the nanoliter per minute range (nL/min) [20] with minimal sample dilution but benefit from the sheath liquid regarding spray formation, ionization process, and flexibility in the selection of the BGE. Examples are a low sheath flow interface with a blunt [21] or tapered stainless steel needle [22], a flow-through microvial using a tapered stainless steel needle [23], a nanoflow sheath liquid interface with a glass emitter [24, 25], and a self-aligning hybrid liquid junction interface with a polished fused silica capillary as emitter [26]. The nanoflow sheath liquid interface using a glass emitter introduced by Hsieh in 1999 [25] was electrically connected by metal wire. Dovichi's group connected the tapered glass emitter of 8–35 μm opening via a cross piece to the electrode in a sheath liquid reservoir at ambient pressure [20, 24, 27] (commercialized as EMASS-II, CMP Scientific, Brooklyn, NY). The outer diameter of the separation capillary end can be reduced by etching to reach further into the emitter tip and minimize analyte diffusion [20]. With this interface, more than 20 applications have been published, mainly in the field of monoclonal antibody (mAb) analysis, proteomics, metabolomics, polysaccharides, and peptide analysis where LODs of picomolar concentrations could be achieved [27–31]. However, comparison with other interfaces has not been performed yet, as also noted by others [6].

In this work, the first systematic comparison of a nanoflow sheath liquid interface to the standard triple-tube sheath liquid and to a sheathless interface for CE-ESI-MS coupling is presented. A nanoflow sheath liquid interface with an etched capillary inside a glass emitter and a sheathless interface using a capillary with a porous tip were selected as representative

interfaces due to the number of publications and reported performance. The experiments were performed under identical conditions applying the same instrumentation, samples, and time frame, using organic acids in negative mode and tryptic peptides and a reduced mAb in positive mode to cover a wide mass range. For the nanoflow sheath liquid interface, the electric and flow characteristics were studied and a syringe pump, shut-off valve, and inline filter enabled fast and repeatable analysis. The same interfacing setup was used to perform both nanoflow sheath liquid and sheathless porous-tip coupling with only minor modifications.

Materials and methods

Chemicals and samples

Methanol, isopropanol (both LC-MS grade), acetic acid, formic acid, sodium hydroxide, and hydrochloric acid were obtained from Carl Roth GmbH und Co. KG (Karlsruhe, Germany). All solutions were prepared using ultrapure water (18 MΩ*cm at 25 °C, SG Ultra Clear UV from Siemens Water Technologies, USA). Hydrofluoric acid 40% (v/v) was purchased from Merck (Darmstadt, Germany). Dithiothreitol (DTT) and sodium bicarbonate were obtained from Sigma-Aldrich (Steinheim, Germany). "ES Tuning mix" solution was obtained from Agilent Technologies (Palo Alto, CA, USA). Dynamic UltraTrol™ low normal (LN) coating was from Target discovery (Palo Alto, CA, USA). Sample solutions of a model mAb (kindly provided by F. Hoffmann-La Roche AG) were used. For the reduction, 1 M DDT was added and, after heating during 5 min at 70 °C in a Thermomixer (Eppendorf, Wesseling-Berzdorf, Germany), the sample was centrifuged at 14,500 rpm for 45 s (MiniSpin plus, Eppendorf, Wesseling-Berzdorf, Germany). Standard mixtures of six organic acids (4-toluenesulfonic acid, 4-styrenesulfonic acid, 1-octanesulfonic acid, 3-nitrobenzenesulfonic acid, naphtalene-2-sulfonic acid, and decane-1-sulfonic acid) obtained from Sigma-Aldrich (Steinheim, Germany) were prepared by solving them in ultrapure water and diluting to final concentrations. The trypsin-digested BSA was from New England Biolabs (Ipswich, USA) and diluted to final concentration in acetonitrile:water (20:80 v/v) with 0.01% (v/v) formic acid.

Nanoflow CE-MS interface

The setup of the nanoflow interface is shown in Fig. 1. A separation capillary is threaded through a PEEK T-union with a 1.3-mm ID (Upchurch Scientific, Munich, Germany) into a borosilicate electrospray emitter of 5.5-cm length, 1-mm OD, 0.75-mm ID, and 3-mm tapered tip, finishing in a 30-μm

Fig. 1 Schematic representation of both nanoflow interfacing setups. Syringe with pump (**a**), 10 μm inline filter (**b**), shut-off valve (**c**), sheath/conductive liquid reservoir with grounding electrode (**d**) nanoflow sheath liquid (**e**), and sheathless porous-tip (**f**) interface. Further information, see "Nanoflow CE-MS interface"
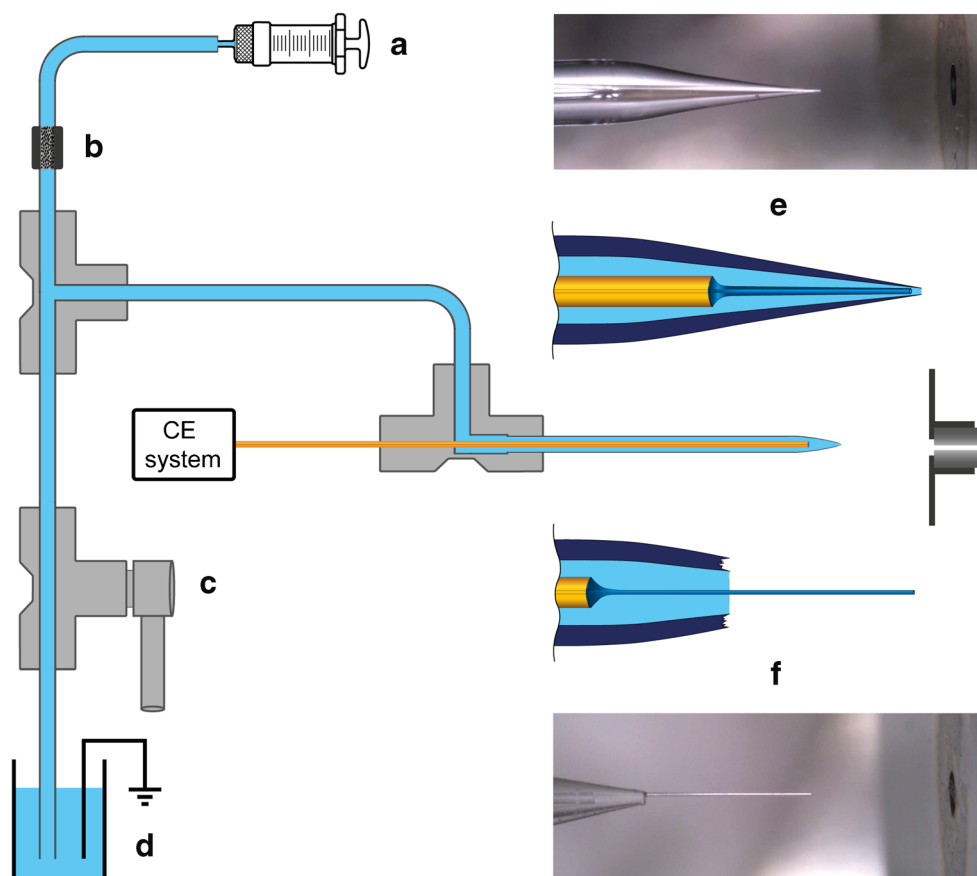
opening (Gynemed, Lensahn, Germany). The capillary outlet of 30- or 50-μm ID and 365-μm OD capillaries (Polymicro Technologies, AZ, USA) was etched with hydrofluoric acid to reduce the outer diameter to a 5–10-μm wall thickness. For sheathless porous-tip applications, capillaries were etched to a 5-μm wall thickness till porosity [9] over approximately 3 cm length and the emitter tip was opened to approximately 100 μm so that the porous capillary tip protrudes approximately 1 cm.

An XYZ-stage allowed positioning of the emitter in front of the MS entrance. A 10-μm inline filter, PEEK T-unions, and PEEK tubing with 0.5-mm ID and 1.6-mm OD were obtained also from Upchurch Scientific. The tubing for sheath or conductive liquid had a total length of 35 cm from the emitter T-union to the reservoir (Fig. 1). A syringe pump (Cole-Parmer®, IL, USA) with a 5-mL syringe (5MDF-LL-GT, SGE Analytical Science, Melbourne, Australia) was used to fill the system with sheath or conductive liquid. Between analyses, the flow to the reservoir was closed by a shut-off valve to flush the emitter (Upchurch Scientific). Emitter tip and spray plume were observed using a digital microscope (HR 5 MP Long distance, Dino-Lite Europe, The Netherlands). For standard sheath liquid experiments, the triple-tube interface (G1607A from Agilent Technologies) was used at a flow rate of 4 μL/min.

CE-MS conditions

CE experiments were performed using a PrinCE Next 850 (Prince Technologies, Emmen, The Netherlands) or an Agilent 7100 (Agilent Technologies). For MS detection, a micrOTOF-Q controlled by micrOTOF control software (Bruker Daltonik, Bremen, Germany) was used. Data processing was performed using the Bruker Compass Data Analysis software (Bruker Daltonik). The conditions employed for each analyte and each CE-MS interface are summarized in Table 1.

Results and discussion

Setup of the nanoflow interfaces

For nanoflow sheath liquid interfacing, a CE capillary is introduced into a glass emitter protruding a PEEK T-union where the third port is connected to a reservoir filled with sheath liquid and a grounding electrode, similar to the EMASS-II (CMP Scientific, Brooklyn, NY) [25, 32]. In the literature, flushing of the separation capillary is performed by applying low pressures with running electrospray [20, 33] leading to long preconditioning times. The implementation

Table 1 Final conditions used for each analyte for the three interfaces

Analyte	Interface	CE conditions					Interface parameters		MS parameters	
		Capillary	BGE	Voltage [kV]	Separation pressure [mbar]	Injection	Sheath/conductive liquid	Distance emitter –MS [mm]	ES potential [V]	Mass range [m/z]
Organic acids	Triple tube	30 μm ID, 365 μm OD, 70 cm	10% (v/v) HAc	−30	–	100 mbar × 20 s	IPA:H₂O (50:50 v/v) with 0.5% (v/v) FAc	–	+3800	50–500
	Nanoflow sheath liquid				–		IPA:H₂O (50:50 v/v) with 0.5% (v/v) FAc	2.0	+900	
	Sheathless porous tip				35		10% (v/v) HAc	2.0	+1100	
mAb	Triple tube	30 μm ID, 365 μm OD, 70 cm (UltraTrol LN coating)	10% (v/v) HAc	+30	–	100 mbar × 20 s	MeOH:H₂O (50:50 v/v) with 0.5% (v/v) FAc	–	−4500	700–3500
	Nanoflow sheath liquid				–		MeOH:H₂O (50:50 v/v) with 0.5% (v/v) FAc	2.0	−1300	
	Sheathless porous tip				100		10% (v/v) HAc	2.0	−1300	
BSA digest	Triple tube	30 μm ID, 365 μm OD, 70 cm	10% (v/v) HAc	+30	–	100 mbar × 20 s	IPA:H₂O (50:50 v/v) with 0.5% (v/v) FAc	–	−4500	200–3000
	Nanoflow sheath liquid				–		IPA:H₂O (50:50, v/v) with 0.5% (v/v) FAc	2.0	−1000	
	Sheathless porous tip				–		10% (v/v) HAc	2.0	−1100	

of a syringe pump in combination with a shut-off valve allows synchronized flushing of sheath liquid and BGE in between analyses. This setup prevents displacement of sheath liquid in the emitter tip by BGE during preconditioning. This leads to reproducible starting conditions also at high capillary inlet pressure to speed up preconditioning and thus reducing total analysis time. Any CE instrumentation and different capillary dimensions can be used.

Figure 1 shows the setup used where the third port of the emitter T-union is connected via a second T-union to a reservoir with a grounding electrode and to a sheath liquid syringe pump for filling and flushing the system free of air bubbles. During analysis, the sheath liquid reservoir is open to ambient pressure for grounding and a free flow of sheath liquid. Between analyses, a shut-off valve locks the path between reservoir and emitter to allow flushing of sheath liquid and electrolyte at the same time. The reservoir and syringe pump are leveled with the emitter tip to prevent hydrodynamic flows generated by siphoning. A 10-μm filter is positioned inline between the syringe pump and second T-union for filtering the sheath liquid to avoid clogging of the emitter tip.

To perform the sheathless experiments, the setup allows switching from nanoflow sheath liquid to sheathless mode by simply exchanging the sheath liquid by conductive liquid and the tip by an emitter with a 100-μm opening so that the capillary can protrude. In this case, capillaries with a porous and electrical conductive tip were used.

Electric and flow characterization of the nanoflow sheath liquid interface

In order to optimize the interface parameter settings and facilitate method development, the involved potentials, currents, resistances, and sheath liquid flow rates during ESI were determined. To achieve a proper electrospray, the potential at the emitter tip is an important value, which is indirectly set by applying potentials at the CE capillary inlet and the MS inlet, respectively. Typical nano electrospray currents appear to be in the range of some hundred nanoamperes and are limited by the rate of charge separation [14, 34]. Consequently, electrospray voltages of around 1–2 kV lead to resistances in the order of several GΩ for electrosprays (Fig. 2 R_{ES}). In contrast, typical separation currents in CE are in the low to mid microampere range. In our setup for the nanoflow sheath liquid interface, as shown in Fig. 2, a current of 6 μA was measured using a BGE of 10% (v/v) acetic acid and a sheath liquid of methanol:water (50:50 v/v) with 0.5% (v/v) formic acid while applying 30 kV at the inlet of a 70-cm-long fused silica capillary with 30 μm ID, resulting in a total resistance of 5 GΩ. Taking the same CE capillary in a CE system where both ends are introduced in BGE vials with electrodes, the measured current increased by around 0.2 μA. This difference implies a certain resistance of the sheath liquid system and a

voltage drop of some hundred volts from capillary outlet to the grounding electrode and therefore a potential located at the emitter tip. By calculating the resistance of the sheath liquid system by using measured values for the specific resistance of individual sheath liquids and the geometry of the sheath liquid system (calculated value for $R_{SL} = 0.08$ GΩ, Fig. 2, for emitter with inserted capillary, T-unions, and tubing), remaining potentials of 0.3 to 0.5 kV are present at the emitter tip. This is in agreement with the fact that the electrospray onset potential at the MS inlet is lowered by 400 V when CE voltage is turned on. It is obvious that the generally higher current in the separation capillary requires a drain for the excess current that is unable to flow over the electrospray which is why the sheath liquid needs to be conductive and determines the remaining potential in the emitter tip. Therefore, the maximum separation current, electrospray voltage, and sheath liquid composition are interdependent and careful optimization is required. This kind of nanoflow interface with a glass emitter has been reported to be electrokinetically driven, with sheath liquid pumped by EOF generated on the emitter surface [28]. The voltage drop of about + 400 V from the capillary outlet to the grounding electrode by applying a positive potential in the CE inlet can generate an EOF only away from the emitter tip, independent of electrospray polarity and independent of location of ES potential (positive needle or negative MS inlet). This fact is generally caused by the higher currents in CE compared to ESI. Consequently, the EOF cannot be the driving force of the sheath liquid flow which is contradictory to previously published statements [28, 35].

So far, flow rate for this type of interface was only estimated [20], however, is of importance in the context of stable and sensitive CE-ESI MS as also noted by others [6]. The flow rate in self-flow nano electrospray is depending on liquid parameters like surface tension, viscosity, conductivity, electric field strength, emitter geometry, orifice diameter, and backpressure [36–39]. To determine the flow rates in the setup, an additional tubing of 0.5 mm ID and 10 cm length filled with sheath liquid was connected horizontally (leveled to prevent siphoning effects) extending the reservoir. The consumption was measured during analysis depending on spray voltage and sheath liquid composition. In negative mode, flow rates of approximately 0.4 µL/min were measured with 900 V MS inlet potential, 2.0 mm distance, and a sheath liquid of isopropanol:water (50:50 v/v) with 0.5% (v/v) formic acid or with 10 mM ammonium acetate. The flow rate increased to 0.8 µL/min with increased distance of the capillary outlet to emitter tip from 0.30 to 0.80 mm without influencing the peak intensity or peak shape (see Electronic Supplementary Material (ESM) Fig. S1). In positive mode, lower flow rates of approximately 0.2 µL/min for methanol:water (50:50 v/v) with 0.5% (v/v) formic acid were determined under optimized conditions.
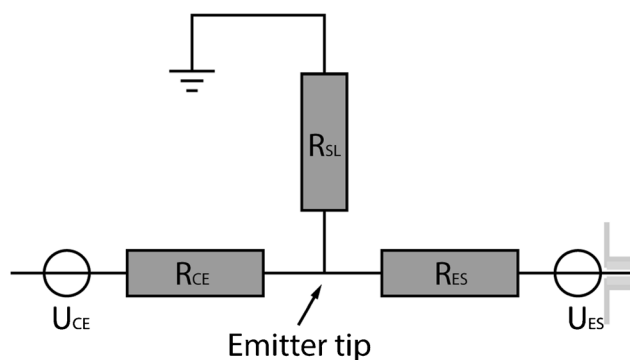
Fig. 2 General scheme for liquid supported electrospray systems for CE-MS with reservoir held on ground with R_{CE}, resistance of the separation capillary; R_{SL}, resistance of the sheath liquid tubing including emitter tip; R_{ES}, resistance of the electrospray. U_{CE} is the applied CE potential and U_{ES} the electrospray potential

Optimization of interfacing parameters

In the following, experiments for the optimization of the interface parameters are described. The final conditions are shown in Table 1.

Distances and electrospray voltage

To study the influence of the distance between emitter tip and MS inlet and the applied electrospray voltage on signal intensity, direct infusion experiments were performed for the nanoflow sheath liquid interface and sheathless porous-tip interface. The separation capillary was filled with a mixture of four organic acids (0.5 µg/mL), the digested BSA (0.225 pmol/µL), or the reduced mAb (0.057 mg/mL) solved in BGE and separation conditions were applied. Intensities of related analyte traces and signal stability were measured in dependency of distance from 0.5 to 4.0 mm and electrospray voltages from 500 to 2000 V in both interfaces. In accordance with the literature, closer distances led to higher signal intensities in the three applications due to more efficient sampling of the electrospray plume [40] but also to lower spray stability [41]. A distance of 2.0 mm between emitter tip and MS inlet offered sensitive and stable spray for both interfaces and was therefore chosen for the final experiments for the comparison of the interfaces. The lowest MS inlet potential, at which the spray was stable, yielded the highest signal intensities for both nanoflow interfaces and all groups of analytes. Stable spray conditions were achieved with approximately 100–200 V more than the onset voltage. These results from the direct infusion experiments were confirmed by separation experiments. For the nanoflow sheath liquid interface, it is important to note that the CE current influences the remaining potential at the emitter tip. Therefore, the spray stability is affected by current fluctuations, e.g., due to high resistivity sample plugs or unstable CE-conditions.

To minimize dead volume and prevent diffusion for the nanoflow sheath liquid interface, it is recommended to reduce the OD of the capillary outlet (Fig. 1). The same etching protocol was used as for the porous-tip capillaries to 5–10 μm wall thickness. By using a microscope, the capillary outlet could be positioned 0.30 mm away from the emitter orifice without impeding the sheath liquid flow. A distance of 0.40 mm did not influence peak width or intensity, whereas distances of 1.5 and 1.2 mm led to significant peak broadening for the sulfonic acids (see ESM Fig. S1) and the light chain (LC) and heavy chain (HC) of the mAb, respectively, corresponding to the distance of a non-etched capillary. Therefore, the precise etching is not as important for the nanoflow sheath liquid as for the porous-tip interface and could be also manufactured by grinding to avoid working with hydrofluoric acid [42].

Sheath liquid composition

The sheath liquid composition was optimized individually for both sheath liquid interfaces and each group of analytes.

For the organic acids, different proportions of isopropanol and methanol to water with formic acid, acetic acid, and ammonium acetate as additives in concentrations of 0.1, 0.2, 0.5, and 2% (v/v) were tested. In contrast to positive mode where methanol:water mixtures are commonly used for the nanoflow sheath liquid interface, in negative mode methanol contents lower than 75% (v/v) can lead to corona discharge for the required onset voltage [4]. However, increasing the methanol content to 75–99% (v/v) reduces the surface tension of the sheath liquid and stable electrospray is possible [43, 44]. All combinations of the different additives with isopropanol:water (50:50 v/v), where the surface tension is similar to mixtures with 85% (v/v) methanol [45], led to a stable spray. For low-conductivity sheath liquids of more than 85% (v/v) methanol with 0.5% formic acid or isopropanol:water (50:50 v/v) with acetic acid content of up to 2% (v/v), onset voltage is reached and electrospray could be initiated when − 30 kV were applied in the CE inlet without MS inlet voltage. Therefore, these sheath liquids are not applicable in this setup since the actual electrospray voltage cannot be controlled. Altering the sheath liquid tubing dimension could minimize this limitation. Further, 10 mM ammonium acetate as basic additive did not improve ionization efficiency in both interfaces. Finally, a mixture of isopropanol:water in 50:50 v/v with 0.5% (v/v) formic acid provided the highest signal intensities for both sheath liquid interfaces. For the reduced mAb, 50% (v/v) methanol or isopropanol in water with 0.2 or 0.5% (v/v) formic acid as sheath liquids were tested for the triple-tube and nanoflow sheath liquid interface, selecting methanol with 0.5% (v/v) formic acid due to the higher intensity observed. In the case of tryptic BSA digest, isopropanol:water (50:50 v/v) with 0.5% (v/v) formic acid provided the highest signal

intensities. In all experiments, the conductive liquid used for electrical contact in the sheathless porous-tip interface was the same as the BGE, which is common practice [15, 41].
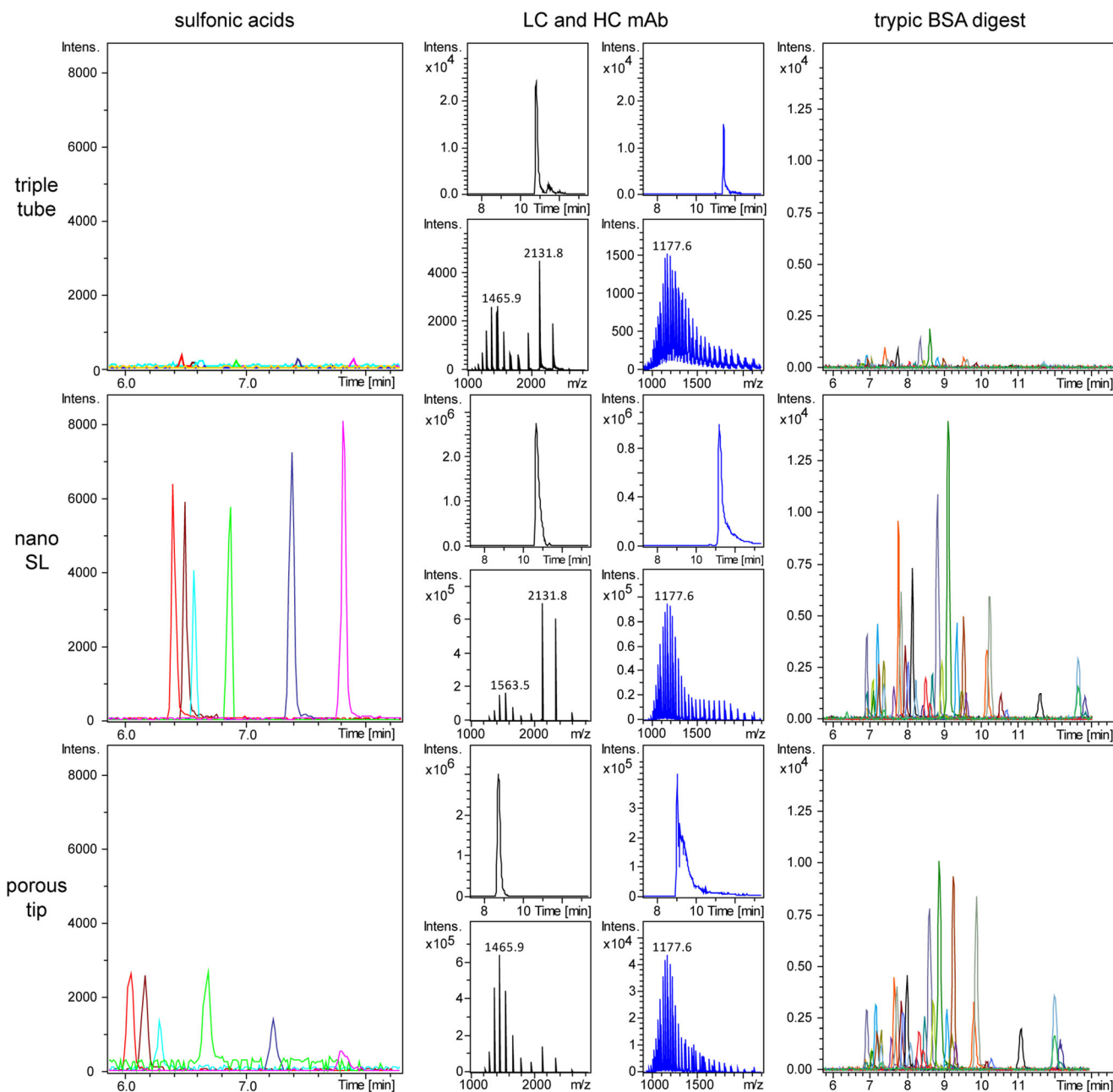
Pressure in sheathless porous-tip interface

The capillary flow in the sheathless porous-tip interface is mainly caused by the EOF and the suction from the ESI process. The latter becomes negligible above a flow rate of 10 nL/min [46]. In the case of mAb analysis, capillaries with a dynamic pre-coating as UltraTrol LN were used to prevent protein adsorption and minimize the EOF. Therefore, an inlet CE pressure is required to create a sufficient flow of BGE to maintain electrospray. With pressures between 10 and 100 mbar (flow rates between 2 and 20 nL/min for a 30-μm ID and 70-cm capillary considering the EOF = 0), no significant differences in signal intensity were observed. Jarvas et al. [47] demonstrated that the signal intensity of an infused mAb stays constant for flow rates between 250 and 20 nL/min. A 100-mbar inlet pressure was selected during experiments for the reduced mAb due to higher spray stability. In the case of the organic acids, bare-fused silica capillaries in combination with reversed polarity (− 30 kV inlet potential) were used and the low EOF with pH of around 2 for 10% (v/v) acetic acid was counterbalanced with a 35-mbar inlet pressure. However, the EOF generated in the MS direction by normal polarity (+ 30 kV) for the tryptic BSA digest was sufficient to sustain a stable spray and no extra pressure was applied in the CE inlet.

Capillary dimensions

Different capillary dimensions have been used so far without showing any limitation or restriction in design for the nanoflow sheath liquid interface [48] which is advantageous for method development. For the sheathless porous-tip interface, Moini suggested in the first experiments in 2007 that a wide range of capillary sizes could be used, but 20–30-μm ID capillaries were especially appropriate [9]. In the commercial sheathless porous-tip interface by Sciex, the dimensions are fixed in length (90 cm), ID (30 μm) [49], and OD (150 μm) by design.

In our experiments, capillaries with 30- and 50-μm IDs were compared in the triple-tube and nanoflow sheath liquid interfaces to study the difference in analytical performance for the reduced mAb. By injecting the same plug length for both capillary diameters (corresponding to threefold lower injected volume for the 30-μm capillary), factors of 1.5 in intensity and 2.0 in area were determined for 50-μm ID capillaries in the triple-tube interface. However, for both IDs used in the nanoflow sheath liquid interface, similar intensities and peak areas were obtained (data not shown). This could be explained by a better ionization efficiency due to a reduced mass flow of BGE with 30-μm ID capillaries [50]. Therefore, depending on

Fig. 3 Comparison of the three different interfaces (in rows: triple-tube, nanoflow sheath liquid interface; sheathless porous-tip interface) for the three analytes selected (in columns: organic acids; reduced mAb; tryptic BSA digest). Organic acids: EIEs for 4-toluenesulfonic acid (#2, *m/z* 171.011), 4-styrenesulfonic acid (#3, *m/z* 183.011), 1-octanesulfonic acid (#5, *m/z* 193.089), 3-nitrobenzenesulfonic acid (#1, *m/z* 201.981), naphthalene-2-sulfonic acid (#4, *m/z* 207.011), decane-1-sulfonic acid (#6, *m/z* 221.121); 0.5 μg/mL in water. mAb: EIEs for HC and LC of reduced model mAb (2.27 mg/mL) in water with the corresponding mass spectra. BSA digest: EIEs for trypsin-digested BSA peptides (0.225 pmol/μL) in acetonitrile:water (80:20, *v/v*) with 0.01% (*v/v*) formic acid. For further conditions, see Table 1

the capillary dimension used in the triple-tube interface, different improvement factors can be expected for the comparison between the interfaces.

Analytical performance of the three interfaces

Comparative analyses between all interfaces were carried out within 2 to 3 days for each group of analytes using the same instrumentation with the previously optimized conditions (Table 1) to minimize deviations in instruments performance. The CE method and MS parameters were not optimized for highest sensitivity, since the comparison was the goal of the study. Factors of improvement for signal intensity and area were determined for both nanoflow interfaces in relation to the triple-tube interface. Reproducibility for one type of interface was tested on two subsequent days with exchanged

Table 2 Factor of improvement, repeatability, and reproducibility for each analyte with the three interfaces

Analyte	Interface	Factor of improvement[a]		Repeatability RSD (%)[b]		Reproducibility RSD (%)[c]	
		Area	Intensity	Area	Intensity	Area	Intensity
Organic acids	Triple tube	1	1	7.4	7.9	10.8	12.0
	Nanoflow sheath liquid	21–59 ($\bar{x} = 38$)	25–44 ($\bar{x} = 35$)	6.6	6.1	11.3	6.8
	Sheathless porous tip	4–22 ($\bar{x} = 12$)	2–12 ($\bar{x} = 11$)	3.5	6.8	–	–
mAb	Triple tube	1	1	13.1	9.0	9.5	12.8
	Nanoflow sheath liquid	114 (LC)/36 (HC)	76 (LC)/34 (HC)	10.2	15.4	16.5	22.2
	Sheathless porous tip	110 (LC)/26 (HC)	87 (LC)/18 (HC)	10.8	9.3	–	–
BSA digest	Triple tube	1	1	24.2	23.0	–	–
	Nanoflow sheath liquid	9–27 ($\bar{x} = 13$)	8–28 ($\bar{x} = 12$)	12.0	12.4	–	–
	Sheathless porous tip	3–31 ($\bar{x} = 10$)	2–26 ($\bar{x} = 6$)	16.8	16.7	–	–

[a] Ratio between values of nanoflow sheath liquid or porous-tip and triple-tube interface, given for concentrations: reduced mAb, 2.27 mg/mL for LC and HC; BSA digest, range and average of 26 peptides from 0.225 pmol/µL; organic acids, range and average of six analytes for 0.5 µg/mL

[b] Repeatability. mAb: triple-tube ($n = 6$, 2.27 mg/mL) and nanoflow sheath liquid ($n = 4$, 2.27 mg/mL), sheathless porous tip ($n = 2$, 2.27 mg/mL). BSA digest: all interfaces ($n = 3$, 0.225 pmol/µL). Organic acids: triple-tube ($n = 3$, 5.0 µg/mL), nanoflow sheath liquid ($n = 3$, 0.5 µg/mL), sheathless porous tip ($n = 2$, 0.5 µg/mL)

[c] Reproducibility. mAb: triple-tube ($n = 10$, 2.27 mg/mL) and nanoflow sheath liquid ($n = 8$, 2.27 mg/mL). Organic acids: triple-tube ($n = 6$, 5.0 µg/mL), nanoflow sheath liquid ($n = 6$, 0.5 µg/mL)

separation capillaries and glass emitters in the case of the nanoflow sheath liquid interface.

For the comparison in negative mode, a mixture of six organic acids was separated within 12 min (Fig. 3). In the case of the nanoflow sheath liquid interface, stable electrospray was achieved without coating of the borosilicate emitter in negative mode, although recommended in a recent publication [4]. Calibration curves were generated from five concentration levels between 200 and 5000 ng/mL for the triple-tube and 8 to 1000 ng/mL for the nanoflow interfaces to compare sensitivity, linearity of response, and LOD for the compounds (see ESM Table S1). In comparison with the triple tube, factors in area for the six analytes in 500 ng/mL samples of 4 to 22 higher for the sheathless porous-tip interface and 21 to 59 higher for the nanoflow sheath liquid interface were achieved. No significant peak broadening was observed for both nanoflow interfaces. The triple-tube and nanoflow sheath liquid interface show good results regarding repeatability and reproducibility (Table 2). No reproducibility data for the sheathless interface are given due to difficulties in the etching process and limited lifetime, though several capillaries were tested.

To compare the three interfaces also in positive mode, a reduced mAb and trypsin-digested BSA were analyzed. The HC and LC were separated in around 10 min (Fig. 3). Both nanoflow interfaces showed significant gains for peak area and intensity compared to the triple-tube interface. Alterations of the obtained LC mass spectra were observed for the three interfaces (see Fig. 3 and ESM Fig. S2). In contrast to sheathless, the charge state distribution is shifted to lower charge state and higher *m/z* in both sheath liquid

interfaces. Several factors can be responsible for this effect such as the concentration of available protons, flow rate (micro- or nanospray regime), electrospray voltage, or the low polarity and higher gas-phase basicity of methanol from the sheath liquid in comparison with water [51, 52]. Mass spectra of the LC at low concentrations (ESM Fig. S2) show better spectra quality for both nanoflow interfaces demonstrating the advantages for analysis of low concentrated samples.

For the tryptic BSA digest (0.225 pmol/µL), average factors in area of 14 and 11 higher for the 26 most intense peaks were observed in the nanoflow sheath liquid interface and sheathless porous-tip interface, respectively (Table 2), as exemplarily shown in Fig. 3. Due to the low concentration used, greater variabilities in signal intensity led to poor repeatability in the triple-tube interface (Table 2). The overall higher sensitivity allowed observation of additional peaks with the nanoflow sheath liquid and sheathless porous-tip interface, showing the advantage of the nanoflow interfaces for sequence coverage where only low concentrated samples in minute volumes are available.

The high signal intensities reached with the nanoflow sheath liquid interface compared to the triple-tube can be mainly explained by a lower sheath liquid flow rate of 20- and 40-fold (flow rates of 4 µL/min for triple-tube and 0.2–0.4 µL/min for nanoflow sheath liquid, see "Electric and flow characterization of the nanoflow sheath liquid interface") and therefore reduced dilution. Moreover, the ionization process is more efficient due to the emitter geometry that causes smaller droplet formation and the closer distance for better sampling. In this context, higher gains would be expected for the sheathless porous-tip interface having a similar emitter

geometry with a low flow rate of around 20 nL/min without dilution. However, the factors obtained with the nanoflow sheath liquid interface were similar. This can be associated with the improved ionization efficiency caused by the sheath liquid. In fact, the use of organic solvents as additive in the BGE can enhance ionization efficiency for a sheathless approach [18, 21], but could interfere with the quality of separation. In the literature, this porous-tip interface has been already compared to the triple-tube interface showing similar factors of improvement as in this work for metabolites and intact proteins [17–19].

Conclusions

In this work, the analytical performance of a nanoflow sheath liquid interface for CE-ESI-MS was compared to standard sheath liquid and sheathless porous-tip interfacing. In research articles where the sensitivity for one interfacing technique is reported in terms of absolute quantities, comparison with others is not ideal because of differences in the applicable conditions and available instrumentation, concealing the real influence of the technique itself. This first comparison was done by keeping most instrument parameters, samples, and time frame constant and covering a wide mass range in positive and negative MS modes in an attempt for fair comparison, despite knowing the difficulty of good and objective methodology.

The triple-tube interface is robust, easy to use, and flexible regarding capillary dimensions, sheath liquid, or BGE selection. Nevertheless, when better analytical sensitivity is required, both nanoflow interfaces demonstrate great benefits both in positive and negative ESI. The performance of the nanoflow sheath liquid interface was similar to the sheathless interface even with the dilution by the sheath liquid. However, sheath liquid-supported systems offer full flexibility in method development due to independence of separation and electrospray conditions that make them more versatile tools. In general, comparable sensitivity could be expected for nanoflow interfaces with similar tip geometry, regardless if sheathless or low-flow sheath liquid supported, remarking that organic modifiers in the electrolyte can enhance ionization for sheathless interfacing for some analytes.

Other key points for the design of new CE-ESI-MS interfaces are handling, reproducibility, and robustness. The characterization of the nanoflow sheath liquid interface adds valuable information for the operation and working principle. The setup used provides a technical solution for reproducible analyses, compatibility with all instrument manufacturers, and ability for high flushing rates of sheath liquid and electrolyte, although the manual handling and fragility still hinder the practicability. Well-engineered and sophisticated parts to simplify assembling for a reasonable price with automated conditioning steps and with the possibility to use standard separation capillaries could be a promising perspective to provide future CE-ESI-MS interfaces to a broader range of users.

Compliance with ethical standards

Conflict of interest The authors declare that they have no conflict of interest.

References

1. Robledo VR, Smyth WF. Review of the CE-MS platform as a powerful alternative to conventional couplings in bio-omics and target-based applications. Electrophoresis. 2014;35:2292–308.
2. Yamamoto M, Ly R, Gill B, Zhu Y, Moran-Mirabal J, BritzMcKibbin P. Robust and high-throughput method for anionic metabolite profiling: preventing polyimide aminolysis and capillary breakages under alkaline conditions in capillary electrophoresis-mass spectrometry. Anal Chem. 2016;88:10710–9.
3. Bonvin G, Schappler J, Rudaz S. Capillary electrophoresis-electrospray ionization-mass spectrometry interfaces: fundamental concepts and technical developments. J Chromatogr A. 2012;1267: 17–31.
4. Sarver SA, Schiavone NM, Arceo J, Peuchen EH, Zhang Z, Sun L, et al. Capillary electrophoresis coupled to negative mode electrospray ionization-mass spectrometry using an electrokinetically-pumped nanospray interface with primary amines grafted to the interior of a glass emitter. Talanta. 2017;165:522–5.
5. Tycova A, Ledvina V, Kleparnik K. Recent advances in CE-MS coupling: instrumentation, methodology, and applications. Electrophoresis. 2017;38:115–34.
6. Heemskerk AAM, Deelder AM, Mayboroda OA. CE-ESI-MS for bottom-up proteomics: advances in separation, interfacing and applications. Mass Spectrom Rev. 2016;35:259–71.
7. Lindenburg PW, Haselberg R, Rozing G, Ramautar R. Developments in interfacing designs for CE–MS: towards enabling tools for proteomics and metabolomics. Chromatographia. 2015;78:367–77.
8. Jarvas G, Guttman A, Foret F. Numerical modeling of capillary electrophoresis—electrospray mass spectrometry interface design. Mass Spectrom Rev. 2015;34:558–69.
9. Moini M. Simplifying CE-MS operation. 2. Interfacing low-flow separation techniques to mass spectrometry using a porous tip. Anal Chem. 2007;79:4241–6.
10. Wang C, Lee CS, Smith RD, Tang K. Ultrasensitive sample quantitation via selected reaction monitoring using CITP/CZE-ESI-triple quadrupole MS. Anal Chem. 2012;84:10395–403.
11. Wang C, Lee CS, Smith RD, Tang K. Capillary isotachophoresis-nanoelectrospray ionization-selected reaction monitoring MS via a novel sheathless interface for high sensitivity sample quantification. Anal Chem. 2013;85:7308–15.

12. Guo X, Fillmore TL, Gao Y, Tang K. Capillary electrophoresis-nanoelectrospray ionization-selected reaction monitoring mass spectrometry via a true sheathless metal-coated emitter Interface for robust and high-sensitivity sample quantification. Anal Chem. 2016;88:4418–25.

13. Nguyen TT, Petersen NJ, Rand KD. A simple sheathless CE-MS interface with a sub-micrometer electrical contact fracture for sensitive analysis of peptide and protein samples. Anal Chim Acta. 2016;936:157–67.

14. Tycova A, Foret F. Capillary electrophoresis in an extended nanospray tip-electrospray as an electrophoretic column. J Chromatogr A. 2015;1388:274–9.

15. Gulersonmez MC, Lock S, Hankemeier T, Ramautar R. Sheathless capillary electrophoresis-mass spectrometry for anionic metabolic profiling. Electrophoresis. 2016;37:1007–14.

16. Haselberg R, de Jong GJ, Somsen GW. Low-flow sheathless capillary electrophoresis-mass spectrometry for sensitive glycoform profiling of intact pharmaceutical proteins. Anal Chem. 2013;85:2289–96.

17. Ramautar R, Busnel J-M, Deelder AM, Mayboroda OA. Enhancing the coverage of the urinary metabolome by sheathless capillary electrophoresis-mass spectrometry. Anal Chem. 2012;84:885–92.

18. Haselberg R, Ratnayake CK, de Jong GJ, Somsen GW. Performance of a sheathless porous tip sprayer for capillary electrophoresis-electrospray ionization-mass spectrometry of intact proteins. J Chromatogr A. 2010;1217:7605–11.

19. Hirayama A, Tomita M, Soga T. Sheathless capillary electrophoresis-mass spectrometry with a high-sensitivity porous sprayer for cationic metabolome analysis. Analyst. 2012;137:5026–33.

20. Sun L, Zhu G, Zhang Z, Mou S, Dovichi NJ. Third-generation electrokinetically pumped sheath-flow nanospray interface with improved stability and sensitivity for automated capillary zone electrophoresis-mass spectrometry analysis of complex proteome digests. J Proteome Res. 2015;14:2312–21.

21. Gonzalez-Ruiz V, Codesido S, Far J, Rudaz S, Schappler J. Evaluation of a new low sheath-flow interface for CE-MS. Electrophoresis. 2016;37:936–46.

22. Choi SB, Zamarbide M, Manzini MC, Nemes P. Tapered-tip capillary electrophoresis nano-electrospray ionization mass spectrometry for ultrasensitive proteomics: the mouse cortex. J Am Soc Mass Spectrom. 2017;28:597–607.

23. Maxwell EJ, Zhong X, Zhang H, van Zeijl N, Chen DDY. Decoupling CE and ESI for a more robust interface with MS. Electrophoresis. 2010;31:1130–7.

24. Wojcik R, Dada OO, Sadilek M, Dovichi NJ. Simplified capillary electrophoresis nanospray sheath-flow interface for high efficiency and sensitive peptide analysis. Rapid Commun Mass Spectrom. 2010;24:2554–60.

25. Hsieh F, Baronas E, Muir C, Martin SA. A novel nanospray capillary zone electrophoresis/mass spectrometry interface. Rapid Commun Mass Spectrom. 1999;13:67–72.

26. Krenkova J, Kleparnik K, Grym J, Luksch J, Foret F. Self-aligning subatmospheric hybrid liquid junction electrospray interface for capillary electrophoresis. Electrophoresis. 2016;37:414–7.

27. Sun L, Zhu G, Yan X, Zhang Z, Wojcik R, Champion MM, et al. Capillary zone electrophoresis for bottom-up analysis of complex proteomes. Proteomics. 2016;16:188–96.

28. Sun L, Zhu G, Yan X, Champion MM, Dovichi NJ. Capillary zone electrophoresis for analysis of complex proteomes using an electrokinetically pumped sheath flow nanospray interface. Proteomics. 2014;14:622–8.

29. Sun X, Lin L, Liu X, Zhang F, Chi L, Xia Q, et al. Capillary electrophoresis-mass spectrometry for the analysis of heparin oligosaccharides and low molecular weight heparin. Anal Chem. 2016;88:1937–43.

30. Dai J, Lamp J, Xia Q, Zhang Y. Capillary isoelectric focusing-mass spectrometry method for the separation and online characterization of intact monoclonal antibody charge variants. Anal Chem. 2018;90:2246–54.

31. Han M, Rock BM, Pearson JT, Rock DA. Intact mass analysis of monoclonal antibodies by capillary electrophoresis-mass spectrometry. J Chromatogr B. 2016;1011:24–32.

32. Peuchen EH, Zhu G, Sun L, Dovichi NJ. Evaluation of a commercial electro-kinetically pumped sheath-flow nanospray interface coupled to an automated capillary zone electrophoresis system. Anal Bioanal Chem. 2017;409:1789–95.

33. Chen D, Shen X, Sun L. Strong cation exchange-reversed phase liquid chromatography-capillary zone electrophoresis-tandem mass spectrometry platform with high peak capacity for deep bottom-up proteomics. Anal Chim Acta. 2018;1012:1–9.

34. Cech NB, Enke CG. Practical implications of some recent studies in electrospray ionization fundamentals. Mass Spectrom Rev. 2001;20:362–87.

35. Dovichi NJ, Wojcik R. Sheath-flow electrospray interface (US 2013/0140180 A1). 2013.

36. Schmidt A, Karas M, Dülcks T. Effect of different solution flow rates on analyte ion signals in nano-ESI MS, or: when does ESI turn into nano-ESI? J Am Soc Mass Spectrom. 2003;14:492–500.

37. El-Faramawy A, Siu KWM, Thomson BA. Efficiency of nano-electrospray ionization. J Am Soc Mass Spectrom. 2005;16:1702–7.

38. Konermann L, Ahadi E, Rodriguez AD, Vahidi S. Unraveling the mechanism of electrospray ionization. Anal Chem. 2013;85:2–9.

39. Gañán-Calvo AM, Rebollo-Muñoz N, Montanero JM. The minimum or natural rate of flow and droplet size ejected by Taylor cone–jets: physical symmetries and scaling laws. New J Phys. 2013;15:33035.

40. Kammeijer GSM, Kohler I, Jansen BC, Hensbergen PJ, Mayboroda OA, Falck D, et al. Dopant enriched nitrogen gas combined with sheathless capillary electrophoresis-electrospray ionization-mass spectrometry for improved sensitivity and repeatability in glycopeptide analysis. Anal Chem. 2016;88:5849–56.

41. Faserl K, Kremser L, Muller M, Teis D, Lindner HH. Quantitative proteomics using ultralow flow capillary electrophoresis-mass spectrometry. Anal Chem. 2015;87:4633–40.

42. Tycova A, Prikryl J, Foret F. Reproducible preparation of nanospray tips for capillary electrophoresis coupled to mass spectrometry using 3D printed grinding device. Electrophoresis. 2016;37:924–30.

43. Cole RB, Harrata A. Solvent effect on analyte charge state, signal intensity, and stability in negative ion electrospray mass spectrometry; implications for the mechanism of negative ion formation. J Am Soc Mass Spectrom. 1993;4:546–56.

44. Smith DPH. The electrohydrodynamic atomization of liquids. IEEE Trans Ind Appl. 1986;IA-22:527–35.

45. Vazquez G, Alvarez E, Navaza JM. Surface tension of alcohol water + water from 20 to 50 degree C. J Chem Eng Data. 1995;40:611–4.

46. Heemskerk AAM, Busnel J-M, Schoenmaker B, Derks RJE, Klychnikov O, Hensbergen PJ, et al. Ultra-low flow electrospray ionization-mass spectrometry for improved ionization efficiency in phosphoproteomics. Anal Chem. 2012;84:4552–9.

47. Jarvas G, Fonslow B, Yates JR, Foret F, Guttman A. Characterization of a porous nano-electrospray capillary emitter at ultra-low flow rates. J Chromatogr Sci. 2017;55:47–51.

48. Sun L, Zhu G, Mou S, Zhao Y, Champion MM, Dovichi NJ. Capillary zone electrophoresis-electrospray ionization-tandem mass spectrometry for quantitative parallel reaction monitoring of peptide abundance and single-shot proteomic analysis of a human cell line. J Chromatogr A. 2014;1359:303–8.

49. Zhang W, Hankemeier T, Ramautar R. Next-generation capillary electrophoresis-mass spectrometry approaches in metabolomics. Curr Opin Biotechnol. 2017;43:1–7.

50. Wahl JH, Goodlett DR, Udseth HR, Smith RD. Use of small-diameter capillaries for increasing peptide and protein detection sensitivity in capillary electrophoresis-mass spectrometry. Electrophoresis. 1993;14:448–57.

51. Banerjee S, Mazumdar S. Electrospray ionization mass spectrometry: a technique to access the information beyond the molecular weight of the analyte. Int J Anal Chem. 2012;2012:282574.

52. Iavarone AT, Jurchen JC, Williams ER. Effects of solvent on the maximum charge state and charge state distribution of protein ions produced by electrospray ionization. J Am Soc Mass Spectrom. 2000;11:976–85.